AIAA JOURNAL
Vol. 33, No. 6, June 1995

Investigation of Natural Frequencies and Mode Shapes of Buckled Beams

A. H. Nayfeh* and W. Kreider†
Virginia Polytechnic Institute and State University, Blacksburg, Virginia 24061
and
T. J. Anderson‡
Memphis State University, Memphis, Tennessee 38152

The linear modes of vibration of buckled beams are investigated analytically and experimentally. Assuming a static buckled shape corresponding to the *n*th buckling mode, an exact solution is obtained for the linear modes and associated frequencies of initially buckled beams with fixed-fixed, fixed-hinged, and hinged-hinged boundary conditions. The analytical solution for a first-mode buckled beam is validated experimentally for the fixed-fixed case. The analytically obtained natural frequencies are in excellent agreement with those obtained experimentally. These exact linear modes provide a basis from which to study the nonlinear vibrations of buckled beams.

Introduction

A NUMBER of studies have investigated the nonlinear vibrations of buckled beams. Burgreen[1] and Eisley[2] considered only one mode for a simply supported beam and assumed the shape of this mode. In a different approach, Tseng and Dugundji[3] considered two modes for a clamped beam and assumed that these modes could be expressed as a linear combination of the first two linear buckling modes. In more recent studies by Min and Eisley,[4] Yamaki and Mori,[5] and Afaneh and Ibrahim,[6] three modes were considered. These investigations assumed that the modes of a buckled beam could be expressed in terms of the linear modes of a straight beam with corresponding boundary conditions.

The common thread in the previous work is that the exact linear problem associated with the nonlinear vibrations of buckled beams was not treated before examination of the nonlinear problem. Instead, the modes of vibration for the nonlinear problem were assumed to be related to the modes from other linear problems. Thus, the goal of this work is to provide an exact solution to the linear problem associated with the vibrations of buckled beams and to validate it experimentally. The results can then be used to provide a more accurate framework from which to approach the nonlinear problem.

Problem Formulation

The analytical solution begins with the following nonlinear equation of motion for an undamped, unforced beam that undergoes stretching[7]:

$$m\frac{\partial^2\tilde{w}}{\partial\tilde{t}^2}+EI\frac{\partial^4\tilde{w}}{\partial\tilde{x}^4}+\left[P-\frac{EA}{2\ell}\int_0^\ell\left(\frac{\partial\tilde{w}}{\partial\tilde{x}}\right)^2\mathrm{d}\tilde{x}\right]\frac{\partial^2\tilde{w}}{\partial\tilde{x}^2}=0 \quad (1)$$

In Eq. (1), $\tilde{w}$ is the transverse deflection of the beam, $\tilde{x}$ is the distance along the undeflected beam, $\tilde{t}$ is time, and the tilde indicates a dimensional variable. Other dimensional parameters are the beam length ℓ, the beam's mass per unit length m, Young's modulus E, the beam's cross-sectional area A, the area moment of inertia of the beam cross section I, and the applied axial load P.

Received April 2, 1994; presented as Paper 94-1683 at the AIAA 35th Structures, Structural Dynamics, and Materials Conference, Hilton Head, SC, April 18–20, 1994; revision received July 1, 1994; accepted for publication July 6, 1994.

*University Distinguished Professor, Department of Engineering Science and Mechanics. Fellow AIAA.
†Graduate Student, Department of Engineering Science and Mechanics. Student Member AIAA.
‡Assistant Professor, Department of Mechanical Engineering.

The first step in using Eq. (1) to investigate the linear vibration of buckled beams is to solve the following linear buckling problem subject to appropriate boundary conditions for the critical Euler buckling loads and mode shapes:

$$EI\frac{\mathrm{d}^4\tilde{w}}{\mathrm{d}\tilde{x}^4}+P\frac{\mathrm{d}^2\tilde{w}}{\mathrm{d}\tilde{x}^2}=0 \quad (2)$$

Next, we increase the axial load P beyond the nth critical buckling load $P^{(n)}$ and assume that the postbuckling displacement is $b\phi_n$, where b is a dimensional scaling constant and ϕ_n is the nth buckling mode shape. Hence, we assume that the contributions of all buckling modes other than the nth mode are negligible. Substituting this displacement into Eq. (1) and dropping the time derivative, we obtain the following equation for b:

$$\left[P-P^{(n)}-\frac{EAb^2}{2\ell}\int_0^\ell\left(\frac{\mathrm{d}\phi_n}{\mathrm{d}\tilde{x}}\right)^2\mathrm{d}\tilde{x}\right]b\frac{\mathrm{d}^2\phi_n}{\mathrm{d}\tilde{x}^2}=0 \quad (3)$$

It follows from Eq. (3) that either $b=0$ (unbuckled case) or b is given by

$$b^2=2\ell[P-P^{(n)}]/EA\int_0^\ell\left(\frac{\mathrm{d}\phi_n}{\mathrm{d}\tilde{x}}\right)^2\mathrm{d}\tilde{x} \quad (4)$$

Because $P>P^{(n)}$, Eq. (4) yields the amplitude b of the nth buckling mode.

Having solved the postbuckling problem, we assume that the beam deflection is the sum of the static buckled displacement $b\phi_n(\tilde{x})$ corresponding to the nth buckling mode and a time-dependent relative deflection $\tilde{u}(\tilde{x},\tilde{t})$; that is,

$$\tilde{w}(\tilde{x},\tilde{t})=b\phi_n(\tilde{x})+\tilde{u}(\tilde{x},\tilde{t}) \quad (5)$$

Furthermore, to capture the linear vibrations, we assume that the deflection $\tilde{u}(\tilde{x},\tilde{t})$ is small relative to the static deflection $b\phi_n(\tilde{x})$. For convenience, the resulting equation is rewritten in terms of the following nondimensional variables:

$$u=\frac{\tilde{u}}{\ell},\qquad x=\frac{\tilde{x}}{\ell},\qquad t=\sqrt{\frac{E}{m}}\tilde{t} \quad (6)$$

As a result, the linear vibrations of a beam around its nth buckled mode are governed by the following integrodifferential equation:

$$E\ell^2\frac{\partial^2u}{\partial t^2}+\frac{EI}{\ell^2}\frac{\partial^4u}{\partial x^4}+P^{(n)}\frac{\partial^2u}{\partial x^2}=\frac{EAb^2}{\ell^2}\phi_n''\int_0^1\phi_n'\frac{\partial u}{\partial x}\mathrm{d}x \quad (7)$$

where the primes indicate derivatives taken with respect to x.

To find the natural frequencies and mode shapes from Eq. (7), we employ separation of variables by assuming a time-harmonic solution. Thus, we let

$$u(x,t) = \Phi(x)e^{i\omega\tilde{t}} \tag{8}$$

where ω is the dimensional natural frequency. Now, Eq. (7) becomes

$$\frac{-m\omega^2\ell^4}{EI}\Phi + \Phi^{iv} + \frac{P^{(n)}\ell^2}{EI}\Phi'' = \frac{BAb^2}{I}\phi_n'' \tag{9}$$

where

$$B = \int_0^1 \phi_n'\Phi'\,dx \tag{10}$$

and Φ and ω are the mode shape and natural frequency for any solution that also satisfies the boundary conditions.

Analytical Solutions

To find the general solution of Eq. (9), we treat the definite integral as a constant B; thus, we have a nonhomogeneous linear ordinary differential equation. Hence, its general solution can be expressed as a linear combination of homogeneous and particular solutions; that is,

$$\Phi(x;\omega) = \Phi_h(x;\omega) + \Phi_p(x;\omega) \tag{11}$$

The homogeneous solution can be expressed as

$$\Phi_h = C_1\sin(\lambda_1 x) + C_2\cos(\lambda_1 x) + C_3\sinh(\lambda_2 x) + C_4\cosh(\lambda_2 x) \tag{12}$$

where

$$\lambda_1, \lambda_2 = \left\{\pm\frac{P^{(n)}\ell^2}{2EI} + \frac{1}{2}\sqrt{\left[\frac{P^{(n)}\ell^2}{EI}\right]^2 + \frac{4m\omega^2\ell^4}{EI}}\right\}^{\frac{1}{2}} \tag{13}$$

and the various C_i are arbitrary constants.

Substituting Eq. (11) into Eqs. (9) and (10), we obtain

$$-\frac{m\omega^2\ell^4}{EI}\Phi_p + \Phi_p^{iv} + \frac{P^{(n)}\ell^2}{EI}\Phi_p'' - \frac{Ab^2}{I}\phi_n''\int_0^1 \phi_n'\Phi_p'\,dx = \frac{Ab^2}{I}\phi_n''\int_0^1 \phi_n'\Phi_h'\,dx \tag{14}$$

There are two possibilities:

$$\int_0^1 \phi_n'\Phi_h'\,dx = 0 \tag{15}$$

and hence $\Phi_p = 0$, and the mode shape is given by homogeneous solution, Eq. (12), unless $\Phi_h \equiv 0$. Second

$$\int_0^1 \phi_n'\Phi_h'\,dx \neq 0 \tag{16}$$

and hence $\Phi_p \neq 0$, which depends on the C_i and the functional form of ϕ_n''.

Now that the mode shape Φ is determined in terms of λ_1, λ_2, and the C_i, we enforce the boundary conditions to obtain an eigenvalue problem for ω that consists, in general, of a system of five algebraic equations. Considering a first-mode buckled beam, we investigate this eigenvalue problem for three sets of boundary conditions.

Fixed-Fixed Boundary Conditions

For fixed-fixed conditions, the first buckling load and corresponding mode shape are given by

$$P^{(1)} = \frac{4\pi^2 EI}{\ell^2}, \qquad \phi_1 = 1 - \cos(2\pi x) \tag{17}$$

Hence, Eq. (14) becomes

$$\frac{-m\omega^2\ell^4}{EI}\Phi_p + \Phi_p^{iv} + 4\pi^2\Phi_p'' - \frac{8Ab^2\pi^3}{I}\cos(2\pi x) \times \int_0^1 \sin(2\pi x)\Phi_p'\,dx = \frac{8Ab^2\pi^3}{I}\cos(2\pi x)\int_0^1 \sin(2\pi x)\Phi_h'\,dx \tag{18}$$

It follows from Eq. (18) that the particular solution Φ_p can be expressed as $C_5\cos(2\pi x)$ where C_5 is a constant. Requiring this particular solution to satisfy Eq. (18) yields

$$\left(\frac{8Ab^2\pi^4}{I} - \frac{m\omega^2\ell^4}{EI}\right)C_5 = \frac{8Ab^2\pi^3}{I}\int_0^1 \sin(2\pi x)\Phi_h'\,dx \tag{19}$$

Substituting for Φ_h from Eq. (12) into Eq. (19) yields

$$\left(\frac{8Ab^2\pi^4}{I} - \frac{m\omega^2\ell^4}{EI}\right)C_5 = \frac{8Ab^2\pi^3}{I}\left\{C_1\lambda_1\left[\frac{2\pi(\cos\lambda_1 - 1)}{\lambda_1^2 - 4\pi^2}\right] - C_2\lambda_1\left(\frac{2\pi\sin\lambda_1}{\lambda_1^2 - 4\pi^2}\right) + C_3\lambda_2\left[\frac{2\pi(1-\cosh\lambda_2)}{\lambda_2^2 + 4\pi^2}\right] - C_4\lambda_2\left(\frac{2\pi\sinh\lambda_2}{\lambda_2^2 + 4\pi^2}\right)\right\} \tag{20}$$

Now, we enforce the following fixed-fixed boundary conditions:

$$\Phi = \Phi' = 0 \quad \text{at} \quad x = 0 \quad \text{and} \quad 1 \tag{21}$$

Substituting $\Phi = \Phi_h + C_5\cos(2\pi x)$ into Eqs. (21) and using Eq. (12), we obtain

$$\begin{bmatrix} 0 & 1 & 0 & 1 \\ \lambda_1 & 0 & \lambda_2 & 0 \\ \sin\lambda_1 & \cos\lambda_1 & \sinh\lambda_2 & \cosh\lambda_2 \\ \lambda_1\cos\lambda_1 & -\lambda_1\sin\lambda_1 & \lambda_2\cosh\lambda_2 & \lambda_2\sinh\lambda_2 \end{bmatrix} \times \begin{Bmatrix} C_1 \\ C_2 \\ C_3 \\ C_4 \end{Bmatrix} = \begin{Bmatrix} -C_5 \\ 0 \\ -C_5 \\ 0 \end{Bmatrix} \tag{22}$$

Considering Eq. (13), we conclude that Eqs. (20) and (22) are five homogeneous algebraic equations that define an eigenvalue problem for the C_i and the natural frequency ω.

Again, there are two possibilities. First, the right-hand side of Eq. (19) or equivalently Eq. (20) is zero and hence $C_5 = 0$. Second, the right-hand side of Eq. (20) is different from zero and hence $C_5 \neq 0$. For $C_5 \neq 0$, the eigenvalue problem yields natural frequencies as eigenvalues that depend upon the initial buckled deflection. For $C_5 = 0$, the eigenvalue problem reduces to a system of four homogeneous algebraic equations that can be obtained from Eq. (22) by letting $C_5 = 0$. The resulting eigenvalues are independent of the initial buckled deflection. Having found the natural frequencies as eigenvalues, we can easily substitute these eigenvalues back into Eqs. (20) and (22) to yield the mode shapes.

To illustrate the results of the solution previously described, we calculate the natural frequencies and mode shapes for a beam subjected to a range of initial deflections b. In particular, we consider a steel beam with the following constant dimensions: 0.75 in. in width, 0.0327 in. in thickness, and 10.991 in. in length. These dimensions are chosen for later comparison to the experimental results.

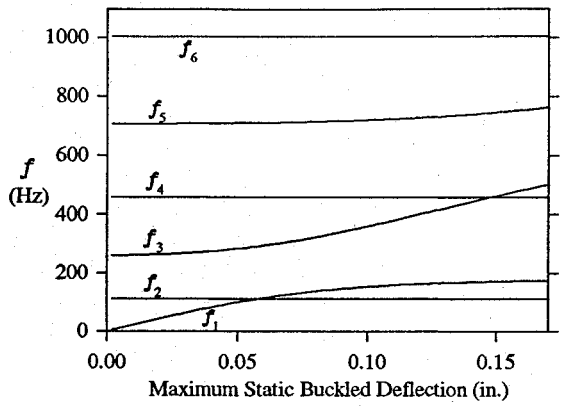

Fig. 1 Natural frequencies vs maximum buckled deflection: fixed-fixed.

In Fig. 1, the first six natural frequencies are plotted vs the initial buckled deflection. From this plot, we note that the second, fourth, and sixth natural frequencies are independent of the initial buckled deflection, whereas the first, third, and fifth increase with the initial buckled deflection. Similarly, the even mode shapes are independent of the initial buckled deflection, whereas the odd ones change with the initial buckling level, as depicted in Fig. 2. These two types of modes correspond to the solutions for which $C_5 = 0$ and $\neq 0$, as noted earlier.

Fixed-Hinged Boundary Conditions

For these boundary conditions, the first buckling load and mode shape are

$$P^{(1)} = \frac{\Omega_1^2 EI}{\ell^2}$$
$$\phi_1 = 1 - x + K\sin(\Omega_1 x) - \cos(\Omega_1 x) \tag{23}$$

where $K \approx 0.2225$ and $\Omega_1 \approx 4.4934$. Equation (14) now becomes

$$-\frac{m\omega^2\ell^4}{EI}\Phi_p + \Phi_p^{iv} + \Omega_1^2\Phi_p''$$
$$-\frac{\Omega_1^2 Ab^2}{I}[-K\sin(\Omega_1 x) + \cos(\Omega_1 x)]$$
$$\times \int_0^1 [-1 + K\Omega_1\cos(\Omega_1 x) + \Omega_1\sin(\Omega_1 x)]\Phi_p'\,dx$$
$$= \frac{\Omega_1^2 Ab^2}{I}[-K\sin(\Omega_1 x) + \cos(\Omega_1 x)]$$
$$\times \int_0^1 [-1 + K\Omega_1\cos(\Omega_1 x) + \Omega_1\sin(\Omega_1 x)]\Phi_h'\,dx \tag{24}$$

From Eq. (24), it follows that the particular solution is $C_5\sin(\Omega_1 x) + C_6\cos(\Omega_1 x)$. Requiring each term of the particular solution to satisfy Eq. (24) yields two equations analogous to Eq. (19) from the fixed-fixed case. From these equations, C_5 is determined in terms of C_6 such that

$$C_5 = -KC_6 \tag{25}$$

Now, requiring the first term of the particular solution $C_5\sin(\Omega_1 x)$ to satisfy Eq. (24) while using Eq. (25) and evaluating the definite integrals yields

$$\left\{\frac{\Omega_1^2 Ab^2}{I}\left[\frac{\Omega_1^2}{2}(1+K^2) - 1 - K\sin\Omega_1 + \cos\Omega_1\right.\right.$$
$$\left. + K\Omega_1\sin^2\Omega_1 + \frac{(K^2-1)\Omega_1}{4}\sin(2\Omega_1)\right]$$
$$\left. - \frac{m\omega^2\ell^4}{EI}\right\}C_5 = -\frac{\Omega_1^2 Ab^2 K}{I}\int_0^1 [-1 + K\Omega_1\cos(\Omega_1 x)$$
$$+ \Omega_1\sin(\Omega_1 x)]\Phi_h'\,dx \tag{26}$$

where

$$\int_0^1 [-1 + K\Omega_1\cos(\Omega_1 x) + \Omega_1\sin(\Omega_1 x)]\Phi_h'\,dx$$
$$= C_1\left[K\Omega_1\lambda_1\left(\frac{\lambda_1\cos\Omega_1\sin\lambda_1 - \Omega_1\sin\Omega_1\cos\lambda_1}{\lambda_1^2 - \Omega_1^2}\right)\right.$$
$$\left. - \sin\lambda_1 + \Omega_1\lambda_1\left(\frac{\lambda_1\sin\Omega_1\sin\lambda_1 + \Omega_1\cos\Omega_1\cos\lambda_1 - \Omega_1}{\lambda_1^2 - \Omega_1^2}\right)\right]$$
$$+ C_2\left[1 - \cos\lambda_1 - \Omega_1\lambda_1\left(\frac{\Omega_1\cos\Omega_1\sin\lambda_1 - \lambda_1\sin\Omega_1\cos\lambda_1}{\lambda_1^2 - \Omega_1^2}\right)\right.$$
$$\left. - K\Omega_1\lambda_1\left(\frac{\Omega_1\sin\Omega_1\sin\lambda_1 + \lambda_1\cos\Omega_1\cos\lambda_1 - \lambda_1}{\Omega_1^2 - \lambda_1^2}\right)\right]$$
$$+ C_3\left[K\Omega_1\lambda_2\left(\frac{\lambda_2\cos\Omega_1\sinh\lambda_2 + \Omega_1\sin\Omega_1\cosh\lambda_2}{\lambda_2^2 + \Omega_1^2}\right)\right.$$
$$- \sinh\lambda_2 + \Omega_1\lambda_2$$
$$\left.\times\left(\frac{\lambda_2\sin\Omega_1\sinh\lambda_2 - \Omega_1\cos\Omega_1\cosh\lambda_2 + \Omega_1}{\lambda_2^2 + \Omega_1^2}\right)\right]$$
$$+ C_4\left[1 - \cosh\lambda_2 + \Omega_1\lambda_2\right.$$
$$\times\left(\frac{\lambda_2\sin\Omega_1\cosh\lambda_2 - \Omega_1\cos\Omega_1\sinh\lambda_2}{\lambda_2^2 + \Omega_1^2}\right)$$
$$\left. + K\Omega_1\lambda_2\left(\frac{\lambda_2\cos\Omega_1\cosh\lambda_2 + \Omega_1\sin\Omega_1\sinh\lambda_2 - \lambda_2}{\lambda_2^2 + \Omega_1^2}\right)\right] \tag{27}$$

Next, we enforce fixed-hinged boundary conditions as

$$\Phi = \Phi' = 0 \quad \text{at} \quad x = 0$$
$$\Phi = \Phi'' = 0 \quad \text{at} \quad x = 1 \tag{28}$$

Substituting $\Phi = \Phi_h + C_5\sin(\Omega_1 x) + C_6\cos(\Omega_1 x)$ into Eqs. (28) and using Eqs. (12) and (25), we have

$$\begin{bmatrix} 0 & 1 & 0 & 1 \\ \lambda_1 & 0 & \lambda_2 & 0 \\ \sin\lambda_1 & \cos\lambda_1 & \sinh\lambda_2 & \cosh\lambda_2 \\ -\lambda_1^2\sin\lambda_1 & -\lambda_1^2\cos\lambda_1 & \lambda_2^2\sinh\lambda_2 & \lambda_2^2\cosh\lambda_2 \end{bmatrix}$$
$$\times \begin{Bmatrix} C_1 \\ C_2 \\ C_3 \\ C_4 \end{Bmatrix} = \begin{Bmatrix} C_5/K \\ -\Omega_1 C_5 \\ -C_5\sin\Omega_1 + C_5\cos\Omega_1/K \\ C_5\Omega_1^2\sin\Omega_1 - C_5\Omega_1^2\cos\Omega_1/K \end{Bmatrix} \tag{29}$$

At this point, the solution can be obtained as in the case of fixed-fixed boundary conditions. The system of five homogeneous algebraic equations (26) and (29) constitute an eigenvalue problem for the C_i and the natural frequency ω.

Again, there are two possibilities. First, the right-hand side of Eq. (26) is zero and therefore $C_5 = 0$. Second, the right-hand side is different from zero and hence $C_5 \neq 0$. For these boundary conditions, the right-hand side of Eq. (26) is different from zero for all solutions to the homogeneous problem. Hence, all modes contain the particular solution and consequently depend on the initial buckled deflection. The dependence of the fist six natural frequencies and first four mode shapes on the buckled deflection is illustrated in Figs. 3 and 4 for the same beam considered in the plots for the fixed-fixed boundary conditions.

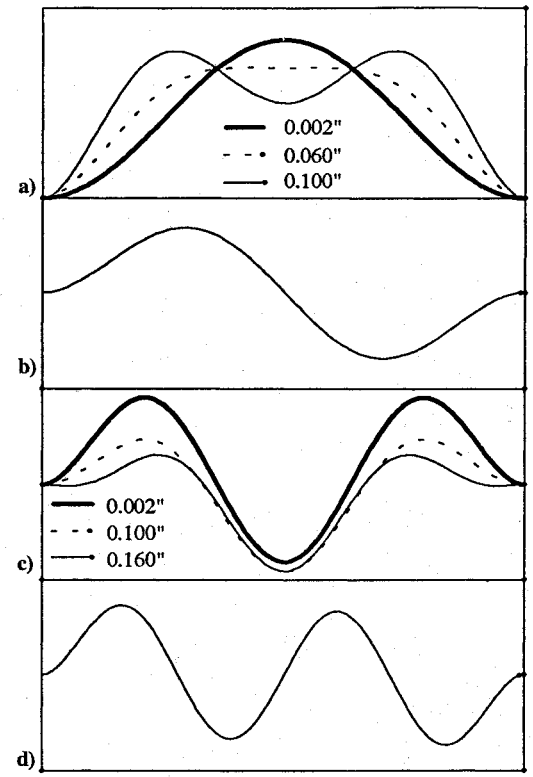

Fig. 2 Mode shapes for a) the first mode, b) the second mode, c) the third mode, and d) the fourth mode are depicted for fixed-fixed boundary conditions (legend indicates maximum buckled deflections in inches).

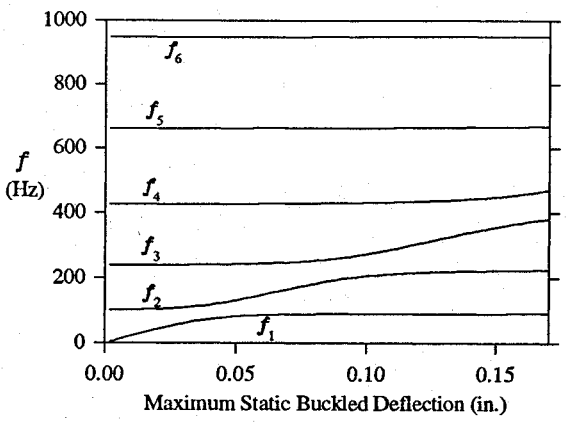

Fig. 3 Natural frequencies vs maximum buckled deflection: fixed-hinged.

Hinged-Hinged Boundary Conditions

For these boundary conditions, the first buckling load and mode shape are

$$P^{(1)} = \frac{\pi^2 EI}{\ell^2}, \qquad \phi_1 = \sin(\pi x) \tag{30}$$

which upon substitution into Eq. (14) yields

$$-\frac{m\omega^2\ell^4}{EI}\Phi_p + \Phi_p^{iv} + \pi^2\Phi_p'' + \frac{Ab^2\pi^3}{I}\sin(\pi x)\int_0^1 \cos(\pi x)\Phi_p' = -\frac{Ab^2\pi^3}{I}\sin(\pi x)\int_0^1 \cos(\pi x)\Phi_h' \, dx \tag{31}$$

The functional form of the right-hand side suggests that the particular solution is $C_5 \sin(\pi x)$. Requiring the particular solution to satisfy Eq. (31) yields

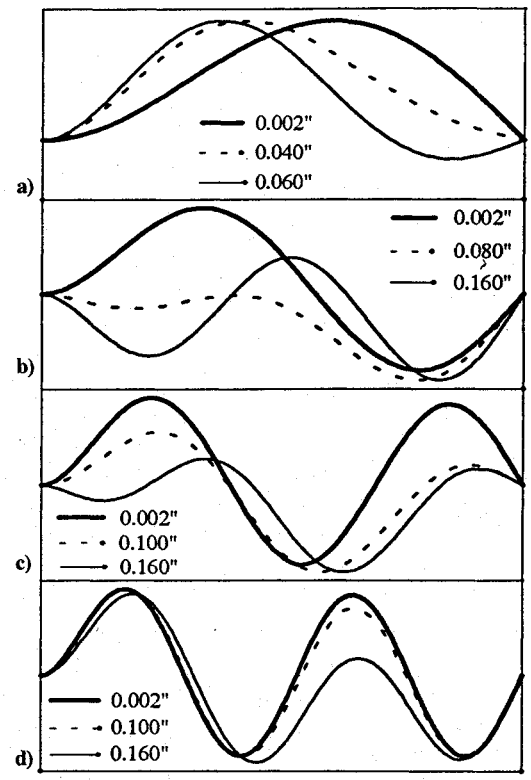

Fig. 4 Mode shapes for a) the first mode, b) the second mode, c) the third mode, and d) the fourth mode are depicted for fixed-hinged boundary conditions (legend indicates maximum buckled deflections in inches).

$$\left(\frac{Ab^2\pi^4}{2I} - \frac{m\omega^2\ell^4}{EI}\right)C_5 = -\frac{Ab^2\pi^3}{I}\int_0^1 \cos(\pi x)\Phi_h' \, dx \tag{32}$$

At this point, we consider the boundary conditions. The hinged-hinged boundary conditions are given by

$$\Phi = \Phi'' = 0 \text{ at } x = 0 \text{ and } 1 \tag{33}$$

Substituting $\Phi = \Phi_h + C_5 \sin(\pi x)$ into Eqs. (33) and using Eq. (12), we have

$$\begin{bmatrix} 0 & 1 & 0 & 1 \\ 0 & -\lambda_1^2 & 0 & \lambda_2^2 \\ \sin\lambda_1 & \cos\lambda_1 & \sinh\lambda_2 & \cosh\lambda_2 \\ -\lambda_1^2\sin\lambda_1 & -\lambda_1^2\cos\lambda_1 & \lambda_2^2\sinh\lambda_2 & \lambda_2^2\cosh\lambda_2 \end{bmatrix} \times \begin{Bmatrix} C_1 \\ C_2 \\ C_3 \\ C_4 \end{Bmatrix} = \begin{Bmatrix} 0 \\ 0 \\ 0 \\ 0 \end{Bmatrix} \tag{34}$$

The boundary conditions (34) and Eq. (32) constitute a set of five homogeneous algebraic equations for the C_i and the natural frequency ω.

Similar to the other boundary conditions, there are two possibilities: the right-hand side of Eq. (32) is either zero or different from zero. However, a solution to the hinged-hinged boundary conditions is $\Phi_h \equiv 0$. For this case, even though the right-hand side of Eq. (32) vanishes, we must consider $\Phi_p \not\equiv 0$ to maintain a nontrivial solution. This solution then yields the first natural frequency and mode shape as a function of the initial buckled deflection from Eq. (32). The other solutions occur when $\Phi_h \not\equiv 0$. To obtain these solutions, we consider the nontrivial homogeneous solutions to Eqs. (34) for which $\omega \neq 0$. All such solutions have derivatives that are orthogonal to $\cos\pi x$. Hence, $C_5 = 0$ from Eq. (32). Finding the nontrivial solutions to Eqs. (34), we obtain modes that are independent of the

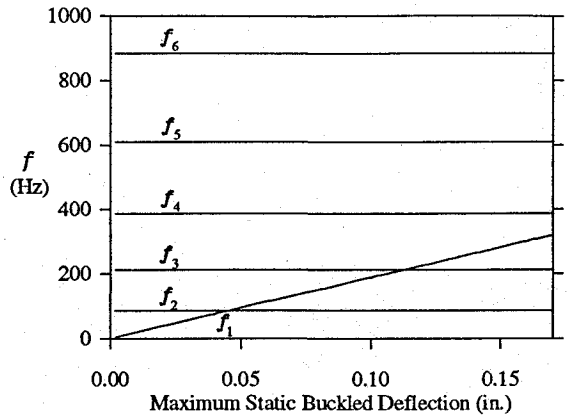

Fig. 5 Natural frequencies vs maximum buckled deflection: hinged-hinged.

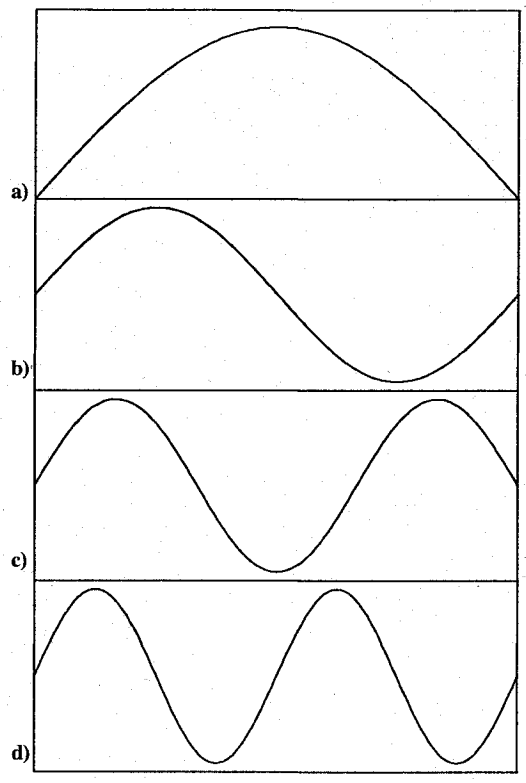

Fig. 6 Mode shapes for a) the first mode, b) the second mode, c) the third mode, and d) the fourth mode are depicted for hinged-hinged boundary conditions.

initial buckled deflection. Thus, for hinged-hinged boundary conditions, the solution may consist of either the particular solution (when $\Phi_h \equiv 0$) or the homogeneous solution (when $C_5 = 0$). Analytical results analogous to those plotted for fixed-fixed and fixed-hinged boundary conditions are presented in Figs. 5 and 6.

Experimental Setup and Results

Experimental data were obtained only for fixed-fixed boundary conditions. The physical setup to the experiment involves a beam (unhardened oil-hardening flat stock) and two clamps, as illustrated in Fig. 7. One of the clamps remains fixed, whereas the other is slotted and is forced to slide by the turning of an adjustment screw. Thus, the adjustment screw provides a controlled method for sliding one of the clamps and buckling the beam. After the beam is buckled, the sliding clamp is also fastened down to complete the simulation of fixed-fixed boundary conditions. The instrumentation includes a laser vibrometer for the beam's response and a hammer with a force transducer for the excitation. Transfer functions were calculated with 512 lines of resolution over a frequency range of

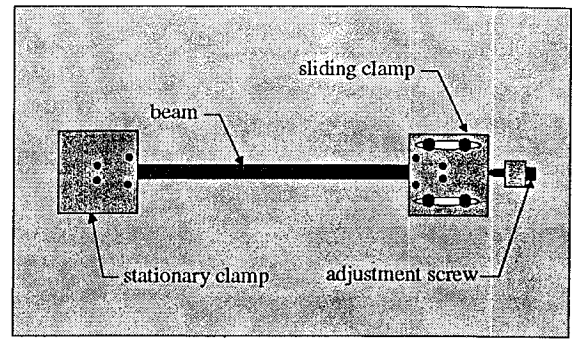

Fig. 7 Top view of the experimental setup.

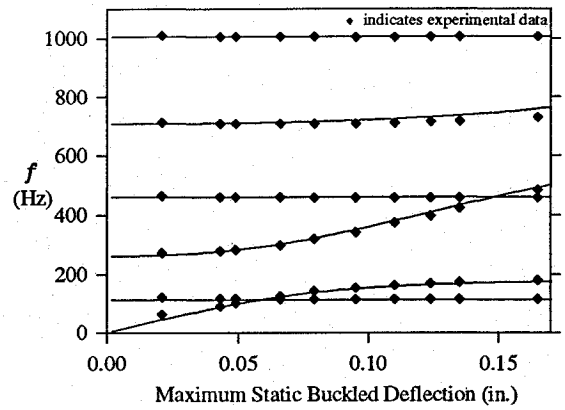

Fig. 8 Experimental and analytical natural frequencies vs maximum buckled deflection.

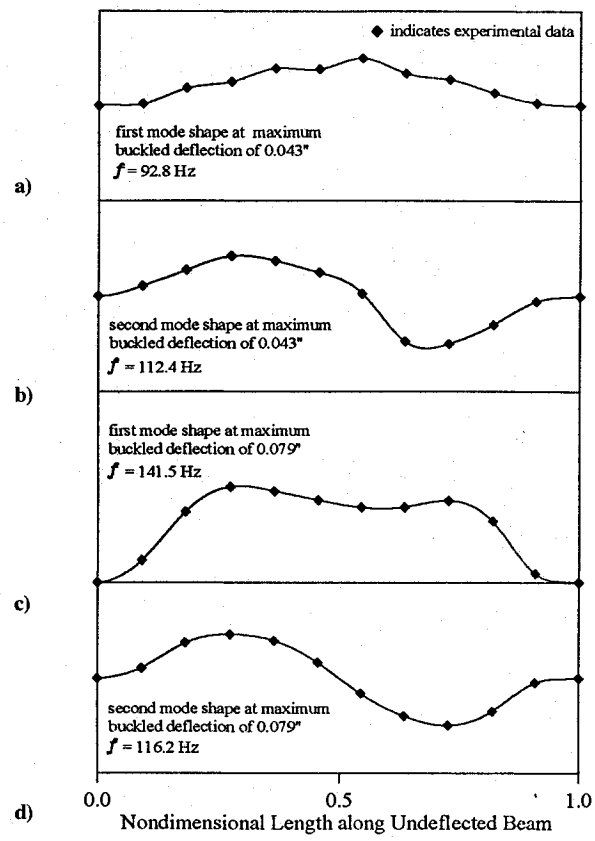

Fig. 9 Experimental mode shapes.

0–1024 Hz. Experimental data were taken at 10 different levels of buckling for which each of the first 6 natural frequencies was determined via a circle fit algorithm. These data points are compared with the analytical results of Fig. 1 in Fig. 8. The same beam parameters are used for the analytical results in both of these figures. The beam thickness of 0.0327 in. is the only parameter in the analytical

model that was adjusted to achieve the excellent agreement shown in Fig. 8. The other parameters were taken to be the actual measured length of 10.991 in. and nominal values for the density and modulus of elasticity of steel. Though the thickness was adjusted slightly to best fit the data, the value used falls well within the range of thicknesses measured along the length of the beam.

In addition to frequency data acquired at multiple levels of buckling, data were taken 10 evenly spaced positions along the beam to investigate mode shapes at 2 levels of buckling, 1 below and 1 above the level at which the 1:1 internal resonance of the first 2 modes occurs. The first and second mode shapes are investigated to verify that the first natural frequency, as defined by mode shape, exceeds the second for levels of buckling greater than that where the 1:1 internal resonance occurs. The exact levels of buckling where the data were taken correspond to maximum initial deflections of 0.043 and 0.079 in. Using a direct parameter fit in MODAL-PLUS software,[8] we confirmed, as shown in Fig. 9, that the first and second natural frequencies do cross between initial deflections of 0.043 and 0.079 in.

Conclusions

The excellent agreement between the analysis and experimental data for fixed-fixed boundary conditions validates the analytical solution. As an exact solution to the linear problem for an nth-mode buckled beam, the modes determined here can then be used in nonlinear studies of buckled beams without the assumption that the modes for this problem are related to the modes from other linear problems. Because the exact modes of a buckled beam vary most from those of a straight beam for large initial buckled deflections, avoidance of mode-shape assumptions gains particular importance at higher levels of buckling.

Acknowledgment

This work was supported by the Air Force Office of Scientific Research under Grant F49620-92-J-0197.

References

[1]Burgreen, D., "Free Vibrations of a Pin-Ended Column with Constant Distance Between Pin Ends," *Journal of Applied Mechanics*, Vol. 18, June 1951, pp. 135–139.

[2]Eisley, J. G., "Large Amplitude Vibration of Buckled Beams and Rectangular Plates," *AIAA Journal*, Vol. 2, No. 12, 1964, pp. 2207–2209.

[3]Tseng, W. Y., and Dugundji, J., "Nonlinear Vibrations of a Buckled Beam Under Harmonic Excitation," *Journal of Applied Mechanics*, Vol. 38, June 1971, pp. 467–476.

[4]Min, G. B., and Eisley, J. G., "Nonlinear Vibration of Buckled Beams," *Journal of Engineering for Industry*, Vol. 94, May 1972, pp. 637–646.

[5]Yamaki, N., and Mori, A., "Nonlinear Vibrations of a Clamped Beam with Initial Deflection and Initial Axial Displacement, Part I: Theory," *Journal of Sound and Vibration*, Vol. 71, No. 3, 1980, pp. 333–346.

[6]Afaneh, A. A., and Ibrahim, R. A., "Nonlinear Response of an Initially Buckled Beam with 1:1 Internal Resonance to Sinusoidal Excitation," *Nonlinear Dynamics*, Vol. 4, No. 6, 1993, pp. 547–571.

[7]Nayfeh, A. H., and Mook, D. T., *Nonlinear Oscillations*, Wiley, New York, 1979, pp. 447–453.

[8]User Manual for Modal Analysis 9.0, General Electric CAE International, MODAL-PLUS Software, 1985.